122 KIEE International Transactions on EMECS, Vol. 3-B, No. 3, pp. 122~127, 2003

3D Transient Analysis of Linear Induction Motor Using the New Equivalent Magnetic Circuit Network Method

Jin Hur*, Gyu-Hong Kang and Jung-Pyo Hong****

Abstract - This paper presents a new time-stepping 3-D analysis method coupled with an external circuit with motion equation for dynamic transient analysis of induction machines. In this method, the magneto-motive force (MMF) generated by induced current is modeled as a passive source in the magnetic equivalent network. So, by using only scalar potential at each node, the method is able to analyze induction machines with faster computation time and less memory requirement than conventional numerical methods. Also, this method is capable of modeling the movement of the mover without the need for re-meshing and analyzing the time harmonics for dynamic characteristics. From comparisons between the results of the analysis and the experiments, it is verified that the proposed method is capable of estimating the torque, harmonic field, etc. as a function of time with superior accuracy.

Keywords: 3D time stepping analysis method, dynamic transient characteristics, induction motor, equivalent magnetic circuit network method

1. Introduction

Predicting the electromagnetic phenomena is essential for motor performance improvement due to the design trends that have been established in recent years. It is also necessary to analyze the motion equation of the armature accurately in order to design their response time. The characteristics of linear induction motors are greatly influenced by the electromagnetic fields at longitudinal and transverse ends of the motors and the end leakage flux at the overhang regions. It is difficult to analyze the dynamic transient characteristics because they require immense computation time and a large memory capacity [1, 5]. Specially, when the motor driven by a PWM inverter is analyzed using the time-stepping 3D method, the number of time steps required to obtain precise results is formidable. Furthermore, the iterative calculations are carried out at each time step to consider the magnetic saturation [2, 6].

In this paper, a new 3D time-stepping method to obtain dynamic transient characteristics by coupling of the external circuit and motion equation is proposed. Its method combines a magnetic equivalent circuit with a numerical method such as FEM. In this method, additional variables like electric potentials are unnecessary because the magneto-motive forces (MMFs) by induced current combine a passive source into the equivalent magnetic circuit network. It also easily takes into account the rotor movement by changing the MMFs and the reluctances in the network without the need for re-meshing. Therefore, the proposed method is capable of modeling the motor 3-dimensionally and analyzing the 3D dynamic characteristic of the motor with less computational time than other 3D analysis techniques like 3D FEM.

The new method is applied to the dynamic transient analysis of the liner induction motor system shown in Fig. 1 to clarify the usefulness of the proposed technique. The results of the developed method are compared with the measurements and also with the 2D analysis result.

2. Characteristic Analysis

2.1 Analysis method

In this paper, the analysis model is divided into hexahedral elements and then an equivalent magnetic circuit network is constructed by connecting the central nodes of the elements to adjacent elements through permeance. After constructing the network using the input current, the geometry and material characteristics of the motor and the influences generated by induced currents are represented as passive components in MMFs and permeance of the conventional network. Therefore, by using only scalar potential at each node, it is possible to model and analyze induction motors in 3-dimensions. Figure 2 shows the mesh shape of LIM. The MMF generated by the induced current can be obtained from Faraday's law as follows:

* Precision Machinery Research Center, Korea Electronic Technology Institute (KETI) Korea. (jinhur@keti.re.kr)
** Dept. of Electrical and Electronic Engineering, Changwon National University, Korea. (kghsjw@hanmail.net, ipmsm@korea.com)
Received: January 4, 2003 ; Accepted: July 14, 2003

$$\nabla\times \vec{E} = -\frac{d\vec{B}}{dt},\quad \nabla\times \vec{J}_e = -\sigma\frac{d\vec{B}}{dt} \tag{1}$$

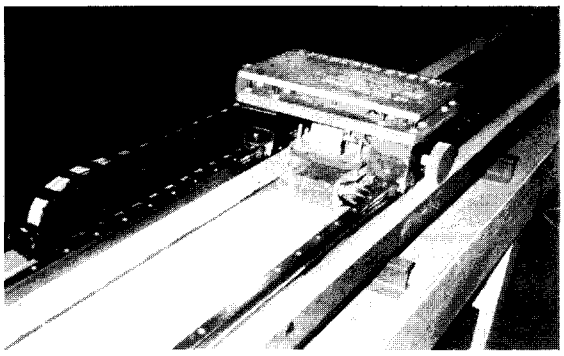

Fig. 1 Prototype of the LIM servo system

The induced current in the conducting region in response to the time varying magnetic flux linked by the region has x- and z-components. From Fig. 2, the differential terms of the above equation can be expressed as the following using the first differential term of Taylor's series.

$$\frac{\partial J_{eu}}{\partial u} = \frac{\Delta J_{eu}}{\Delta u}\bigg|_{u=x,y,z} \tag{2}$$

From (1) and (2), the induced current density may be expressed [8, 9].

$$\begin{aligned} J_{ex} &= P_{x1}\left(-\sigma\frac{dB_x}{dt}\right) + P_{x2}\left(-\sigma\frac{dB_y}{dt}\right) \\ J_{ey} &= P_{y1}\left(\sigma\frac{dB_x}{dt}\right) + P_{y2}\left(\sigma\frac{dB_y}{dt}\right) \\ J_{ez} &= P_{z1}\left(\sigma\frac{dB_x}{dt}\right) + P_{z2}\left(-\sigma\frac{dB_y}{dt}\right) \end{aligned} \tag{3}$$

where $P_{x1} = \Delta x^2\Delta z\left(\Delta y^2+\Delta z^2\right)/K$, $P_{x2} = \Delta x\Delta y\Delta z^3/K$,

$P_{y1} = \Delta x\Delta y\Delta z^3/K$, $P_{y2} = \Delta y^2\Delta z\left(\Delta x^2+\Delta z^2\right)/K$

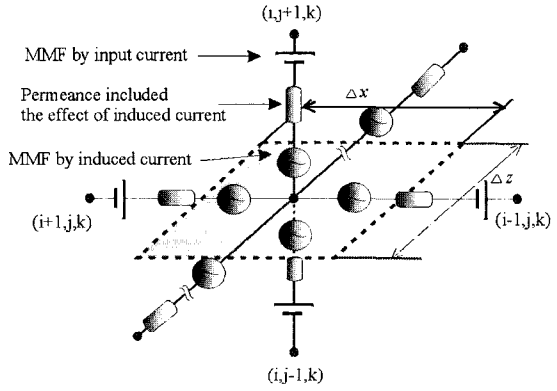

Fig. 2 Flow of magnetic flux at a node and configuration of magnetic circuit network

$$P_{z1} = \Delta x\Delta y^2\Delta z^2/K,\quad P_{z2} = \Delta x^2\Delta y\Delta z^2/K,$$
$$K = \Delta x^2\Delta y^2+\Delta y^2\Delta z^2+\Delta x^2\Delta z^2$$

The conventional reluctance R_m between two nodes is a series connection of two element reluctances, ${R_{m1}}^y$ and ${R_{m2}}^y$ determined by their shape and materials. So, R_m is given by:

$$R_m = {R_{m1}}^y + {R_{m2}}^y = \frac{\mu_0\mu_{r1}\Delta y_{i,j-1,k}+\mu_0\mu_{r2}\Delta y_{i,j,k}}{\mu_0^2\mu_{r1}\mu_{r2}Ay_{i,j,k}} \tag{4}$$

Also, the conventional MMFs by the stator current, $F_S(x)$, is calculated by Ampere's law using a current sheet $J_S(x)$ of three-phase, double-layer distributed winding in the stator such that [5, 6].

$$\begin{aligned} F_S(x) &= \int_0^x J(x)\ dx = \sum_{n=1,3,5}^{\infty}\sum_{n_s=1}^{6}\frac{2NI(n_s)}{n^2k\pi w_s}\cos nk\left(\frac{\tau}{2}-\frac{w_s}{2}\right) \\ &\cdot\left(\cos nk(4t_s-n_st_s)-\cos(x-n_st_s+4t_s)\right) \end{aligned} \tag{5}$$

where n_s is the slot number, $I(n_s)$ is the current of each phase in the slot, k is π/τ and W_s, t_s, τ and N are the slot width, slot pitch, pole pitch and turns in one slot, respectively.

From the constructed conventional equivalent circuit network, the additional reluctance and MMFs are due to the induced current added on the conventional network. The reluctance at the time t can be obtained from (3) as follows:

$${R_{IND}}^y = \frac{\left(\Delta x_{i,j,k}\right)^3\left(\Delta z_{i,j,k}\right)^3}{\left(\Delta x_{i,j,k}\right)^2+\left(\Delta z_{i,j,k}\right)^2}\times 2\ \ \Delta y_{i,j,k}\times\mu_o\mu_{r1}\sigma\frac{\Delta\phi^{t-1}}{\Delta\ t} \tag{6}$$

So, we can achieve new reluctance considering the effect of induced current. Also, the MMFs due to the induced current at the time t can be expressed as:

$${F_{IND}}^t = \frac{\left(\Delta x_{i,j,k}\right)^3\left(\Delta z_{i,j,k}\right)^3}{\left(\Delta x_{i,j,k}\right)^2+\left(\Delta z_{i,j,k}\right)^2}\times 2\ \ \left(\Delta y_{i,j,k}\right)\times\mu_o\mu_{r1}\sigma\frac{\Delta\phi^t}{\Delta\ t} \tag{7}$$

Therefore, the MMFs of the elements in source regions at the time t is:

$${F_{N,(i,j,k)}}^t = \left(\left(F_S(x_{(i,j,k)})+{F_{IND}}^t(x_{(i,j,k)})\right)\Big/ m\right), \tag{8}$$

where m is the number of elements of the teeth and slot

regions in the y direction.

The magnetic flux between two nodes (i,j,k) and $(i,j\text{-}1,k)$ are calculated such that:

$$\phi^{t}_{(i,j,k)} = \frac{1}{R_{N_{(i,j,k)}}} \left(U^{t}_{(i,j,k)} - U^{t}_{(i,j-1,k)} + F^{t}{}_{N_{(i,j,k)}} \right)$$

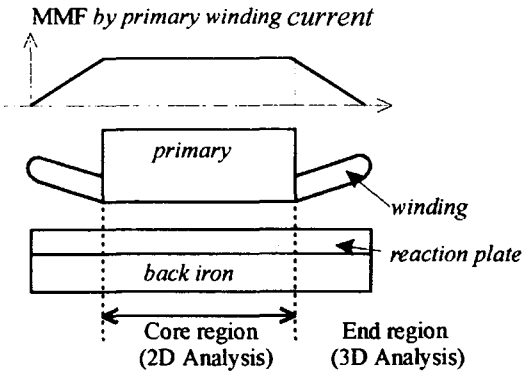

Fig. 3 Modeling of LIM in y-z plane.

$$B_{i,j,k} = \phi_{i,j,k} / Ay_{i,j,k} \tag{9}$$

where, $U^{t}_{(i,j,k)}$ is unknown magnetic scalar potential at node (i,j,k). The permeance is calculated accurately for each divided element.

From (9) and (10), we divided the analysis model into elements and we built the equivalent magnetic circuit network shown in Fig. 1. The MMF due to the end coil is considered as shown in Fig. 3. We can then solve the network using the magnetic continuous condition, which states the sum of inflow and outflow of magnetic flux at node (i, j, k) as:

$$\sum_{i,j,k} \phi^{t}_{(i,j,k)} = 0 \tag{11}$$

Now the equation of the magnetic flux for each direction can be written as:

$$\phi^{t} R^{t}{}_{N} = F^{t}{}_{N} \tag{12}$$

where, $R_N = (R_m + R_{IND})$, $F^{t}{}_{N} = (F_S + F_{IND})$, R_m and F_S are the reluctance and MMF due to input current in conventional MEC and F_{IND} is the induced MMF due to eddy current. Also, we can apply the time diffence method (TDM) to (11). The system matrix equation can be obtained as follows:

$$[\mathbf{P}]_{n\times n} \{\mathbf{U}\}_{n\times 1} = \{\mathbf{F}\}_{n\times 1} \tag{13}$$

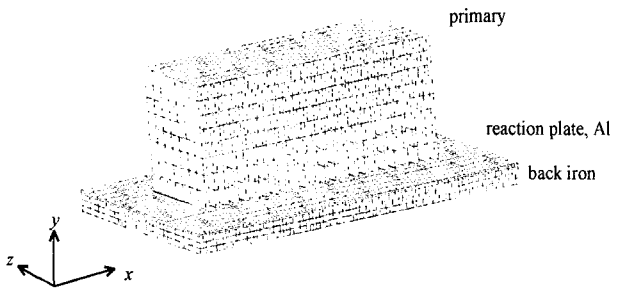

Fig. 4 Mesh shape for EMCN

where n is total number of nodes, $[\mathbf{P}]_{n\times n}$ is the permeance coefficient matrix which is symmetric and has a good sparsity and bandwidth, $\{\mathbf{U}\}_{n\times 1}$ is the matrix of unknown magnetic scalar potential (MSP) at a node, and $\{\mathbf{F}\}_{n\times 1}$ is the forcing matrix including MMF due to the induced current.

2.2 Motion equation and External circuit equation

The motion of the primary is governed by the motion equation,

$$F_{Thrust} - F_{load} = M(dv/dt) + k_f \cdot v \tag{14}$$

where F_{Thrust} is the electromagnetic thrust, M is the mass of mover, v is the mover speed and k_f is the coefficient of viscous friction. When the primary moves from x to $x - x_d$, MMFs distribution of the primary, $F_S(x)$ and the relative permeability $\mu(x)$ of the primary changes at each node for $F_S(x - x_d)$, $\mu(x - x_d)$ according to the moving distance of the mover. As such, the motion of the primary is easily modeled without the need for re-meshing. The external electric circuit equation for one phase of the motor is as follows:

$$V_i = I_i R + N_i \left(\frac{d\Phi_i}{dt} \right) \tag{15}$$

where V_i is the applied input voltage of i-th phase, I_i is the primary current, N_i is the number of turns of primary winding and Φ_i is the primary linked flux.

3. Results and Discussion

The proposed method has been succesfully applied to the study of a LIM. This motor is fed by a three phase voltage source. The total number of nodes and the element

number used for 3D EMCN analysis are 84,940. Results with the proposed method are presented in Figures 5 to 8. Fig. 5(a) shows B_x, B_y and B_z versus x, which are calculated at x-y plane in the center of the air-gap. Fig 5(b) shows B_x, B_y and B_z versus z, which are also calculated at y-z plane in the center of the air-gap.

Compared with the results of 2D analysis assuming that it has a constant value in the z direction, the analysis results indicate that B_y is increasing because of the MMF by end coil and B_z is very large at the end of the core due to lateral leakage flux. The eddy current paths between 2-D and 3-D models are different and the MMFs produced by the end coil are not considered in 2-D analysis. That is, when eddy currents are included in 2-D analysis, error can occur if the leakage fluxes from both sides of the core are not correctly modeled using 2-D analysis. Comparing the proposed method with 2-D FEM respect to the normal force versus time at the locked primary as shown in Fig. 6, the 2-D analysis overestimates the normal force.

It is assumed that the eddy current is constant over the analysis region and the MMF due to the end ring not being included in the 2-D model. So, in order to compensate for the modeling error, the voltage drop of the end ring is only considered by modifiying the conductivity σ in the conventional 2-D formulation [7]. Fig. 7 shows the comparison results of 3-D EMCN and 2-D FEM with compensated conductivity for the thrust according to the time. The currents at standstill are shown in Fig. 8.

References [1-5] reported a similar analysis using 3-D FEM, which required a long computational time of more than two hours for just one time step. Also, for transient simulation, 3-D FEM requires re-meshing at each time step. Therefore, a large computation time is required for time-stepping 3-D transient analysis. However, the proposed method in this paper requires only 10 minutes simulation time for each time step, because it is capable of analyzing

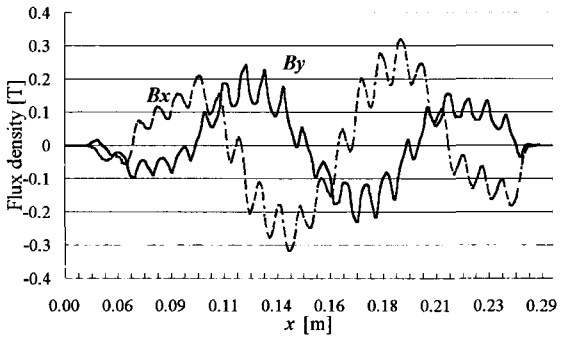

(a) B_x, and B_y versus x at x-y plane
(B_z is zero at the center of the air-gap)

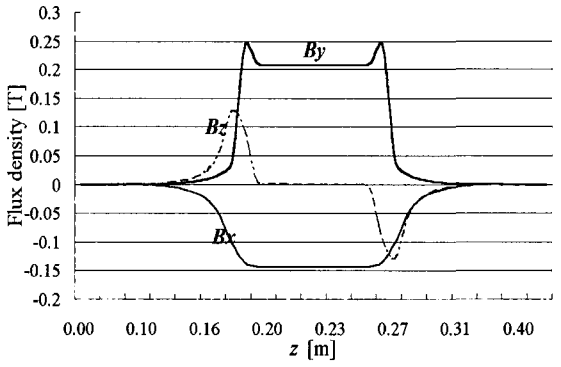

(b) B_x, B_y and B_z versus z at y-z plane

Fig. 5 Distribution of magnetic flux density

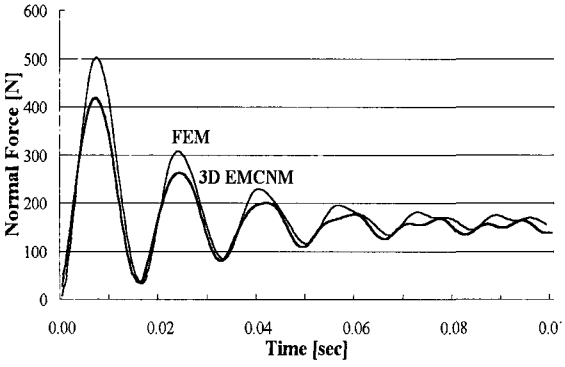

Fig. 6 Normal force versus time
(Comparison of 3-D EMCNM and 2-D FEM)

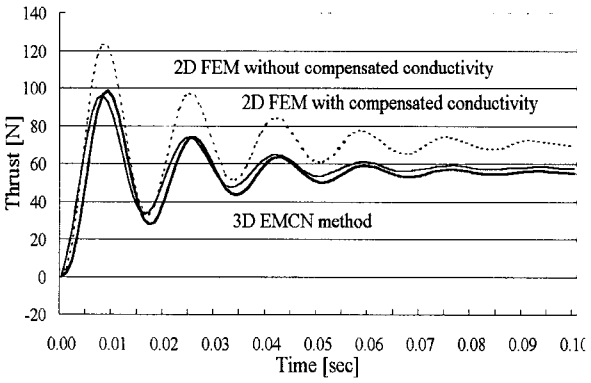

Fig. 7 Thrust versus time

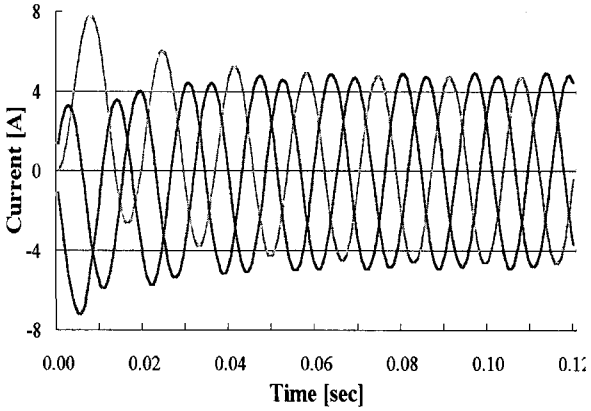

Fig. 8 Currents at standstill

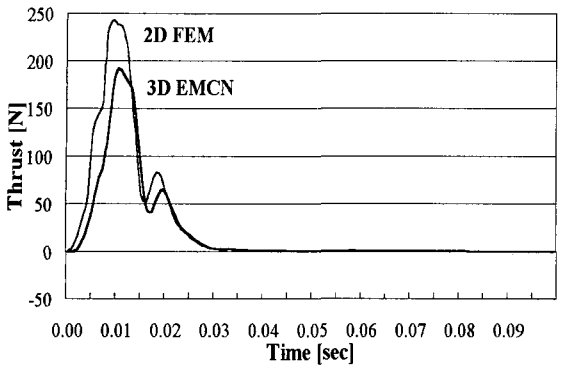

Fig. 9 Comparison for Thrust

the motor without introducing the above mentioned additional variable. Also, this method does not require re-meshing, because the movement is easily modeled by changing the function of the MMF and the reluctance without re-meshing. Therefore, this method is an effective method to analyze transient behavior of an induction motor in 3-D. Fig. 8 shows transient thrust comparing the proposed method with 2-D FEM.

5. Conclusion

In this paper, a new time stepping 3-D numerical method has been proposed for the purpose of analyzing the dynamic transient characteristics of induction motors. This method can analyze induction motor with low computation time for 3-D analysis because it doesn't need additional variables like current vector potential for analyzing the induction current. Accuracy of the method has been successfully tested on a linear induction motor by comparing it with FEM. It must be noted that the low computational time required by the new 3-D simulation of the induction machine has a great advantage over 3-D FEM.

References

[1] T. Yamaguchi Y. Kawase and Y. Hayashi, "Dynamic Transient Analysis for Vector Controlled Motors Using 3-D Finite Element Method," *IEEE Trans. on Magnetics*, Vol. 32, no. 3, pp. 1549-1552, May, 1996.

[2] K. Yamazaki, "Induction Motor Analysis Considering both Harmonics an End Effects using Combination of 2D and 3D Finite Element Method," *IEEE Trans. on Energy Conversion*, Vol. 14, no. 3, pp. 698-703, September, 1999.

[3] P. Dziwniel, and F. Piriou , "A Time-Stepped 2D-3D Finite Element Method for Induction Motors with Skewed Slots Modeling," *IEEE Trans. on Magnetics*, Vol. 35, no. 3, pp. 1262-1265, May, 1999.

[4] A. Yahiaoui and F. Bouillault, "2D and 3D Numerical Computation of Electrical Parameters of an Induction Motor," *IEEE Trans. on Magnetics*, Vol. 30, no. 5, pp. 3690-3692, September, 1994.

[5] J. Hur, Y. D. Chun, J. Lee and D. S. Hyun, "Dynamic Analysis of Radial Force Density in Brushless DC Motor Using 3 Dimensional Equivalent Magnetic Circuit Network Method", *IEEE Trans. on Magnetics*, Vol. 34, no. 5, pp. 3142-3145, September, 1998.

[6] S. B. Yoon, J. Hur and D. S. Hyun, "A Method of Optimal Design of Single-Sided Linear Induction Motor for Transit", *IEEE Trans. on Magnetics*, Vol. 33, no. 5, pp. 4215-4217, November, 1997.

[7] K. H Ha, J. P. Hong, G. T. Kim and T. B. Im, "Finite Elements Analysis of Squirrel-cage Induction Motor Taking into account the End-ring", *KIEE Trans.*, Vol. 48, no. 2, pp. 49-55, 1999.

[8] J. Hur, H. Toliyat and J. P. Hong, "Dynamic Analysis of Linear Induction Motors using 3-D Equivalent Magnetic Circuit Network (EMCN) Method", *Journal of Electric Power Components and Systems*, Vol. 29, No. 6, pp. 531-541, June, 2001.

[9] J. Hur, D. S. Hyun, S. S. Kim, G. H. Kang and J. P. Hong, "Three Dimensional Eddy Current Calculation Using Magnetic Scalar Potential in Conducting Regions," *Journal of Applied Physics*, Vol. 91, No. 10, pp. 8314-8316, May, 2002.

Jin Hur

He received his Ph.D. degree in Electrical Engineering from Hanyang University, Seoul, Korea, in 1999. He was with the Department of Electric Engineering, Texas A&M University, College Station, USA, as a Postdoctoral Research Associate from 1999 to 2000. From 2000 to 2001, he was a Research Professor for BK21 projects with the Dept. of Electric Engineering, Hanyang University. Since 2002, he has been with the Precision Machinery Research Center, KETI as a Managerial Researcher. He is also a senior member of IEEE. His research interests are in design and analysis of high performance electric machines and the numerical analysis of electromagnetic fields.

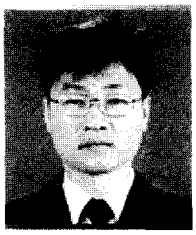

Gyu-Hong Kang

Gyu-Hong kang received his B.S, M.S and Ph.D. degrees from Changwon National University, Changwon, Korea. Between 1994 and 1998, he was employed by LG Electronics Co., Ltd. as a Senior Research Engineer. Since 2001, he was a research Professor for BK21 projects with the Dept. of Electric Engineering, Changwon National University. His research interests are the design of electric machines, coupled problem and numerical analysis of electromagnetics.

Jung-Pyo Hong

Jung-Pyo Hong received his B.S, M.S and Ph.D degrees from Hanyang University, Seoul, Korea. Between 1990 and 1992, he was employed by LG Precision Co., Ltd. as a Research Engineer. Between 1992 and 1995, he was employed by Samsung Electric Co., Ltd. as a Senior Research Engineer. Since 1996, he has been an Associate Professor in the Department of Electric Engineering at Changwon National University, Changwon, Korea. He is also a senior member of IEEE. His research interests are design of electric machines, optimization, coupled problem and numerical analysis of electromagnetics.